From qualitative to quantitative understanding of support effects on the selectivity in silver catalyzed ethylene epoxidation

Catalysis Today 338 (2019) 31–39

Contents lists available at ScienceDirect

Catalysis Today

journal homepage: www.elsevier.com/locate/cattod

From qualitative to quantitative understanding of support effects on the selectivity in silver catalyzed ethylene epoxidation

J.E. van den Reijen[a], W.C. Versluis[a], S. Kanungo[b], M.F. d'Angelo[b], K.P. de Jong[a], P.E. de Jongh[a,*]

[a] Inorganic Chemistry and Catalysis, Debye Institute for Nanomaterials Science, Utrecht University, Utrecht, the Netherlands
[b] Laboratory of Chemical Reactor Engineering, Department of Chemical Engineering and Chemistry, Eindhoven University of Technology, Eindhoven, the Netherlands

ARTICLE INFO

Keywords:
Ethylene oxide
Silver
Heterogeneous catalysis
Kinetic model
Support effects
Epoxidation

ABSTRACT

In the epoxidation of ethylene, catalyzed by supported Ag particles, the support plays not only a beneficial role, but can also negatively impact the selectivity to ethylene oxide. Especially high surface area supports, and supports containing acid groups, seem detrimental for the selectivity, which is attributed to secondary reactions on the support surface. We prepared Ag nanoparticles on supports with a wide range of specific surface areas and different chemical nature, but with similar Ag metal loading and particle size. Indeed, a strong dependence of selectivity on both the specific surface area, and the chemical nature of the oxide support was found, with α-Al_2O_3 giving much more selective catalysts than SiO_2. Furthermore, the conversion was an important factor in determining the selectivity, while on the other hand the support had no influence at all on the ethylene conversion. We described our experimental selectivities with a reaction model that used the rate constant for the secondary reaction of oxidation of ethylene oxide to carbon dioxide and water as the only variable parameter. The model was able to adequately describe the experimental results. It gave insight into the dependence of selectivity on conversion, how the secondary reaction depended on the chemical nature of the support, and how its rate scaled linearly with the support's specific surface area. Building on this insight we modified a SiO_2 support to passivate its OH-groups, which indeed yielded a 94% decrease in the rate of the secondary reaction, performing even better than α-Al_2O_3 with similar specific surface area would. We have shown that the selectivity towards ethylene oxide is dependent on a metal specific, intrinsic selectivity, and the decrease in selectivity with conversion to be support dependent. This decrease is caused by the isomerization of ethylene oxide, which is found to be first order in ethylene oxide and the active sites on the catalyst support.

1. Introduction

Ethylene oxide is a key chemical feedstock, which is produced worldwide on a million-ton scale [1–5]. Every year 16% of the ethylene produced worldwide is converted to ethylene oxide, yielding a compound annual growth rate of 4.3% in the first half of this decade, resulting in a production of 34.5 million ton in 2016 [2]. Ethylene oxide is primarily used to produce ethylene glycol, which is mainly used as antifreeze, but also used in the production of various polymers [1,6,7]. Its synthesis from ethylene is challenging, as full combustion of ethylene leads to the formation of water and carbon dioxide and has to be avoided. Hence, achieving high selectivities is key for a viable process [8,9].

The current industrial process is based upon ethylene oxidation using a silver catalyst discovered in 1931 by Theodor Lefort [10], and industrialized by Union Carbon in 1936 and Shell in 1958 [11–13]. Silver has remained the key component in commercial catalysts, but other components have been added [14]. The original patent of Lefort proposed powdered or colloid silver, but catalysts used in industrial applications nowadays are supported on low surface area α-alumina. Furthermore, they are promoted by a range of metal-based promotors including cesium, and chlorine is continuously co-fed in the gas stream during the process [1,15–17]. These changes resulted in an increased selectivity to ethylene oxide from 68 to 70% for early unpromoted silver catalysts [3], to up to 90% for present industrial catalysts [2,3,18].

As selectivity is key, it is interesting to investigate the reaction paths to ethylene epoxide and CO_2 formation. In 1945 Twigg was the first to propose isomerisation of ethylene oxide to a short lived intermediate, which he proposed was acetaldehyde formed by isomerization of ethylene oxide [19]. Lee et al. showed for a wide range of metal oxide support materials that the support material catalysed the ring opening

* Corresponding author.
E-mail address: p.e.dejongh@uu.nl (P.E. de Jongh).

https://doi.org/10.1016/j.cattod.2019.04.049
Received 30 October 2018; Received in revised form 20 March 2019; Accepted 13 April 2019
Available online 14 April 2019

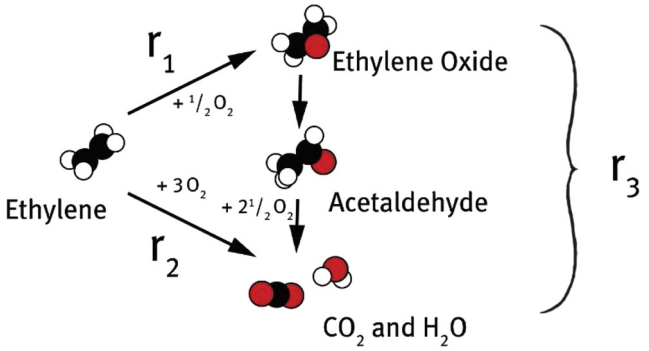

Fig. 1. Proposed reaction scheme for ethylene oxidation over supported silver catalysts comprising several reaction steps. In first instance the ethylene is either selectively oxidized to ethylene oxide, or fully oxidized. The ethylene oxide formed can be recovered as a product but can also undergo consecutive oxidation via a two step-reaction: first the isomerization of ethylene oxide to acetaldehyde over the support and then the oxidation of acetaldehyde to water and carbon dioxide over silver.

of ethylene oxide to form acetaldehyde [20]. However, since acetaldehyde is rarely found under reaction conditions, it is thought that acetaldehyde is rapidly further oxidized to CO_2 in the presence of silver [18,21,22]. This led to a proposed scheme for the silver catalyzed ethylene epoxidation as displayed in Fig. 1 [23].

Selective oxidation of ethylene to ethylene oxide (r_1) competes with full oxidation to CO_2 and H_2O (r_2). Full oxidation is thermodynamically more favorable than selective oxidation (−1323 kJ/mole compared to −106.7 kJ/mole respectively) [1]. The ethylene oxide that is formed can also undergo oxidation (r_3); it is believed that isomerization to acetaldehyde ($r_{3,a}$) is followed by fast further oxidation ($r_{3,b}$). While reactions r_1, r_2 and $r_{3,b}$ are believed to be catalyzed by the metal particle, the isomerization of acetaldehyde is believed to occur on the catalyst support. A common strategy to limit side reactions on the support is minimizing the support specific surface area [22]. Yong, Kennedy and Cant showed a low selectivity towards ethylene oxide for high surface area supports such as titania and γ-alumina and a high selectivity over catalysts supported on low surface area materials [24]. They also reported an influence of the chemical nature of the support. Different rates of ethylene oxide isomerization for α-alumina and for silica supported catalysts were found [24]. This is in agreement with the results from Lee et al. who reported increased rates of ethylene oxide isomerization over acidic supports, with silica and α-alumina yielding higher selectivities and the α-alumina catalyst outperforming the silica supported catalyst [20].

Apart from limiting the support surface area, and choosing a favourable support chemistry, another strategy is to tune the surface properties of a given support. Industrial catalysts contain caesium, which passivates acidic surface groups and limits the isomerization of ethylene oxide to acetaldehyde [17,22,25,23]. During preparation of the catalyst, caesium is co-impregnated with silver, and is therefore not only present on the support surface, but also decorates the silver surface [1,17,26]. Özbek and van Santen showed that caesium also influences the reactivity of the active metal surface, as higher caesium concentration leads to lower overall conversion [20,25,27–29]. Although caesium generally improves the selectivity, in high concentrations it can even lead to lower overall selectivies, probably because caesium introduces oxygen vacancies on the silver surface, which are known to be active sites for full combustion [15,27]. It is clear that if one wants to study intrinsic support effects, promotors such as caesium should rather be avoided.

An open question that is seldomly addressed in academic open literature is the strong dependence of selectivity on conversion, the exact nature of this dependence and how it can be described [10,30,31]. Industrial sources report a linear decrease of selectivity with increasing conversion, based on empirical observations, without offering insight into the origin of this relationship [32–35]. It was proposed that the isomerization of ethylene oxide would be a first order reaction in ethylene oxide and dependent on the support [21,23,36]. The isomerization rate of ethylene oxide in the absence of ethylene was determined, but either only on bare support materials or with catalysts prepared using a variety of preparation methods, with a wide range of silver particle sizes and in the presence of (potential) promotors [20–24,36–38].

To address this important question, we set out to show the effect of the support properties and understand the empirical correlation between conversion and selectivity, by carefully excluding effects due to differences in particle size, metal loading or the presence of promotors. To this aim we prepared series of catalysts on supports with different specific surface areas and surface groups, but having similar silver particle size and weight loading, and being prepared using the same metal precursor. The catalytic performance was described using a kinetic model, enabling us to quantify the impact of the support material on the selectivity, and understanding the correlation between conversion and selectivity in the ethylene epoxidation reaction [32,36]. An experiment in which silanol surface groups were blocked by organic capping agents demonstrated the strength of this approach to limit the secondary reactions and increased the overall selectivity of the reaction.

2. Methods

2.1. Catalyst preparation

A selection of fumed silica supports was obtained from Safic-Alcan Necarbo, specifically Aerosil OX-50, Aerosil 200, Aerosil 300, Aerosil 380, Aerosil R812 and Aerosil R972 (all produced by Evonik). These materials primarily differ by their specific surface area, except the latter two which are silylated versions of Aerosil 300 and Aerosil 150 respectively. A hydrophilic equivalent of Aerosil R812 was obtained after heat treatment of this material in a flow of oxygen (GHSV = 2000 h^{-1}) at 400 °C for 2 h to remove the organic capping agents. The hydrophilic analogue is expected to be equivalent to Aerosil 300. Quartz was supplied by Sigma Aldrich (≥99.995% trace metals basis). 1 m^2/g and 8 m^2/g α-alumina were obtained from Sigma-Aldrich (1 m^2/g; 0.006 cm^3/g; -100 mesh, Sigma Aldrich) and BASF (8 m^2/g; pore volume 0.02 cm^3/g, AL4196E, BASF) respectively. All support materials were pressed and sieved into a 38–90 μm sieve fraction prior to impregnation.

20 m^2/g α-alumina was prepared using a procedure described before [39]. In a typical synthesis 1.5 g of PMMA colloidal crystal powder made by emulsion polymerization of methyl methacrylate (MMA, 99%, ≤30 ppm 4-methoxyphenol inhibitor, Sigma-Aldrich) was placed in a Buchner funnel and drop-wise wetted with approximately 3 mL solution of 1 M aluminum nitrate nonahydrate in demineralized water/methanol (1:1 vol ratio) and soaked for 2 min. Thereafter the excess solution was removed by applying vacuum for 20 min resulting in a dry powder. The powder was wetted with ammonia/methanol (1:1 vol ratio) after which the excess solution is removed via vacuum suction and the sample was dried for 20 min. These steps were repeated three times before drying the powder overnight at room temperature. The dried powder was calcined at 1150 °C under a nitrogen flow with a gas hourly weight velocity (GHWV of at least 20 $L g_{powder}^{-1}$ hr^{-1} for 6 h after a 5 °C/min heating ramp followed by a second calcination in a flow of oxygen with a GHWV of at least 20 L g_{powder}^{-1} hr^{-1} at 1150 °C for 6 h after a 5 °C/min heating ramp.

All catalysts were prepared by incipient wetness impregnation. Support materials were dried for 24 h at 120 °C in a static oven in air. This was sufficient to remove adsorbed water from the macroporous pores of the alumina and from hydrophobic silica materials. For the hydrophilic silica some water was retained in the sample.

Silver oxalate was prepared by adding a 20 mL, 12 M aqueous

solution of silver nitrate (99 + %, Sigma-Aldrich) to a 40 mL, 12 M aqueous solution of oxalate dihydrate (99.5%, Merck) at 60 °C and filtrating and washing the precipitate with miliQ water [31,40–42]. A solution of 0.82 mmol/gram freshly prepared $Ag_2C_2O_4$ in a mixture of ethylene diamine (*en*) and water (0.73 g/g milliQ/(*en*), or 1:4:16 mol ratio $Ag_2C_2O_4$: *en* : H_2O) was used to impregnate the support materials. In the case of hydrophobic supports a mixture of ethylene diamine, water and ethanol was used in a volumetric ratio of 20 : 55 : 25 (*en* : water : ethanol) to ensure wetting of the support. The volume of solution added corresponded to the total pore volume as obtained from nitrogen physisorption. During impregnation, the solution was added dropwise to the dry support material which was continuously mixed to ensure a homogenous distribution of the silver salt over the support. The impregnated material was put in an oven at 60 °C in static air for 12 h to dry. After 5, 10 and 30 min the material was thoroughly mixed to limit macroscopic inhomogenities [43].

The dry grains were heated in a U-shaped reactor to decompose the silver salt, forming a catalyst with 15 wt% silver and an average particle size of 60 nm. In typical heat treatment, 200 mg of sample was heated with a 5 °C/min ramp to a temperature between 215 and 300 °C in an oxygen or nitrogen atmosphere with a gas hourly weight velocity of 120 L g^{-1} hr^{-1} in order to obtain the desired particle size [31]. All catalysts had a nominal weight loading of 15 wt% of silver, but due to the different support specific surface area the silver surface density ($Ag/m^2_{support}$) differs greatly between the catalysts, an estimation of the silver surface density is given in the Supporting information section C and Table S1.

2.2. Characterization

Nitrogen physisorption isotherms for all support materials were measured at −196 °C on a Micromeritics TriStar 3000 apparatus. The specific surface area of the support was calculated by fitting experimental data with the BET equation ($0.05 < p/p^\circ < 0.25$). BJH pore size distributions were obtained from the corresponding adsorption isotherm, with the total pore volume at a relative pressure of 0.995. For the high surface area α-alumina mercury porosimetry was performed using Micromeritics AutoPore IV 9500 to probe the large pores of the material. Pore volume data was calculated over the range 0.0007–227.5270 MPa. The contact angle between the support materials and the mercury was assumed to be 130° and the mercury surface tension and density 0.485 N/m and 13.5335 g/mL, respectively.

The size and spatial distribution of the obtained silver particles were measured using scanning electron microscopy (SEM). The images were obtained using a FEI XL30 FEG SEM. The images were processed using iTEM Soft Imaging System software [44]. Diffuse-Reflectance UV/Vis spectra of the supported silver catalysts were measured using a Varian CARY 500 Scan UV/Vis-NIR spectrophotometer with an integrating sphere. In a typical analysis, 30 mg of analyte was diluted with 600 mg pristine α-Al_2O_3 (1 m2 g^{-1}, -100 mesh, Sigma Aldrich) and ground to a fine powder before taking a spectrum in the 1000 – 200 nm range. A background measurement of pristine α-Al_2O_3 was taken and subtracted from the obtained spectrum. Crystal phase analysis was performed with a Bruker D8 Phaser diffractometer (X-Ray Diffraction, Bruker D8 Phaser diffractometer equipped with a Co Kα source (λ = 0.1789 nm) using an angle range from 20° to 90° in 2θ and comparing XRD patterns with the PDF-4 + 2016 database.

The weight loss due to burning of the organic capping agents from the hydrophobic silicas was analyzed using a Perkin Elmer Pyris 1 TGA under a 10 mL min^{-1} flow of 20% oxygen in nitrogen. For these experiments the temperature was increased from 50 °C to 900 °C with a ramp of 5 °C min^{-1}. The decomposition products were analyzed using a Pfeiffer Vacuum OmniStar mass spectrometer.

2.3. Catalytic testing

In a typical catalysis experiment, 50–150 mg of catalyst grains (38–90 μm) was loaded in a quartz reactor between two layers of quartz wool. To activate the catalyst, the sample was heated to 180 °C in a flow of 16.5 mL min^{-1} of 8.5% oxygen and 30% ethylene in helium. The gas hourly weight velocity (GHWV) per gram of silver was varied over the 25–160 L g_{Ag}^{-1} hr^{-1} range in order to obtain ethylene conversions in the range of 0–10 % (after a stable conversion was obtained), and thus operate in differential conditions. The reaction products were characterized using online gas chromatography. The outlet gases of the reaction were analyzed every 15 min by an online Compact GC (Interscience) equipped with a Porabond Q column and a Molsieve 5 Å column in two separate channels, both with a thermal conductivity detector. Conversion data were calculated from data retrieved after steady state was reached, which was typically after 8 h. A more detailed description of the calculations can be found in the Supporting information (Supporting information section E).

2.4. Kinetic model describing selectivity trends

The overall reaction was modelled based on the reaction scheme presented in Fig. 1. A primary selectivity is determined by the ratio between two parallel paths for the oxidation of ethylene: selective oxidation forming the desired product ethylene oxide (r_1) and full oxidation to form carbon dioxide and water (r_2). The ethylene oxide can either be retrieved, or oxidized further in the reactor (r_3) via the isomerization to acetaldehyde [19,36]. For the oxidation reactions r_1, r_2, that are assumed to occur over the silver nanoparticles, quite some information is available in literature.

Regarding r_1, the partial oxidation of ethylene to ethylene oxide, the reaction is taken to be first order in ethylene, which is a logical assumption, but also experimentally reported by Campbell et al. for experimental conditions similar to ours [45]. The reaction order in oxygen is taken as 0.5, being in the range of -0.5 to 1.5 as reported by Stegelmann et al. [46]. Furthermore both reaction orders are in line with the results of Linic and Barteau [47].

For the full combustion of ethylene (r_2) a reaction order in oxygen in the -1 to 1 range, and typically close to zero, is reported by several different authors [46,48,49]. This zeroth order in oxygen might appear at first sight surprising, given the consumption of oxygen in this reaction. However, it is the combination of both a negative and a positive dependence on the oxygen partial pressure. The positive order stems from the consumption of oxygen in the reaction, but it is balanced by the fact that a more oxidized silver surface favors selective oxidation instead of full combustion [27]. Stegelmann et al. observed the ethylene reaction order in r_2 lower than the ethylene order in r_1 and is taken by us as $^1/_2$ [46].

Because both the r_2 and r_3 yield carbon dioxide and water at equal stoichiometry, it is not straightforward to derive the individual values from the overall catalytic data. Deconvolution of these rate constants was performed by extrapolating the obtained catalytic data of all measured catalysts to a conversion of 0.04% ethylene. At such low conversion, the ethylene oxide partial pressures is close to zero, and isomerization of this component, and hence r_3, can be neglected. The resulting selectivities are therefore governed by the ratio between r_1 and r_2. Hence the rates for r_1 and r_2, and the corresponding rate constants k_1 and k_2, were calculated from the ratio r_1/r_2 and the overall reactant conversion rate (r_1+r_2) at the extrapolated conversion of 0.04%.

Using the obtained rate constants k_1 and k_2 and the experimental feed concentration as the initial conditions, the rates and partial pressures of each component were calculated differentially over the catalyst bed. In each step the result of the previous calculation was used, with initially values defined by the feed composition. The conversion and selectivity were calculated for each step based on the calculated partial

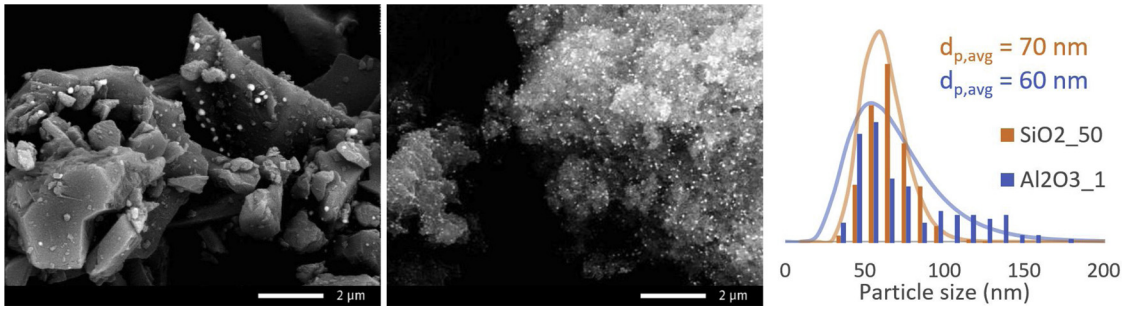

Fig. 2. Electron microscopy images of silver on an α-Al_2O_3 support with a support specific surface area of 1 m^2/g (Al_2O_3_1, left), silver on a fumed silica support with a support specific surface area of 50 m^2/g (SiO_2_50, middle) and histogram of the diameter of the silver particles on both catalysts. These histograms are obtained from measuring at least 300 particles and are subsequently normalized to accurately compare the distributions.

pressures at increasing catalyst bed lengths. A comparison of the calculated selectivities and the real experimental selectivities in the ethylene conversion range of 0–10 % allowed to derive the rate r_3 and corresponding rate constant k_3 for the isomerization of ethylene oxide to acetaldehyde, which was the sole fitting parameter. This value for k_3 for each individual catalyst. rate was obtained by a sum of least squares fit. The secondary reaction as represented by r_3 and k_3 is the process that determines the dependence of overall selectivity on support properties, and the correlation between conversion and selectivity, and is hence the main topic of this study.

3. Results

3.1. Catalyst preparation and characterization

Catalysts in this paper are coded via the method of *Support_surface area*, i.e. Al_2O_3_1 is a sample of α-alumina of 1 $m^2\,g^{-1}$ impregnated with silver and SiO_2_380 is a sample of fumed silica of 380 $m^2\,g^{-1}$ impregnated with silver. In Fig. 2 typical Scanning Electron Microscopy (SEM) images of a low surface area α-alumina and a low surface area fumed silica supported silver catalysts are shown. The support material is visible as a grey material, dotted with bright white silver metal particles. The Al_2O_3_1 catalyst in the left image is supported on large jagged chunks of non-porous material. The silica support (middle frame) has a fine structure and appears to have smaller silver particles than the α-alumina supported catalyst. The histogram (obtained from measuring at least 300 particles) in the right frame shows that the average particle size is only slightly different (surface area corrected average particle size of 70 nm for Al_2O_3_1 compared to 60 nm for SiO_2_50), while the size distribution (fitted as a log-normal distribution) is significantly broader on the former, with some particles with sizes of 100–150 nm being present. The apparent difference between the silver particle sizes in the left and middle frame is due to these large particles being more noticeable.

The large crystallites, in the case of the α-alumina support, can be explained by the preparation method of the support materials, as they are produced at high temperatures to crystallize to the most thermally stable α-alumina phase (at least 1000 °C before α-alumina is formed), causing a collapse of most of the material porosity and condensing surface groups [50–52]. The silica support is prepared by sintering small silica spheres (5–50 nm in diameter) into an agglomerate which has no defined shape and exhibits interparticle nanoporosity [53]. The temperature at which this flame hydrolysis is performed determines the support specific surface area, but does not reach the temperatures needed to crystallize the silica [53]. XRD (see Figure A1 in the Supporting information) confirms the highly crystalline nature of the α-alumina and the amorphous nature of the fumed silica.

An overview of the main characteristics of the silver catalysts and the different support materials used, is given in Table 1. The α-alumina and quartz support materials exhibit low specific surface areas and therefore a low amount of surface hydroxyl species per gram of material. The α-alumina supports have surface areas ranging from 1 to 20 m^2/g, with the highest specific surface area belonging to a non-commercial ordered macroporous α-alumina that was made in-house [39]. Quartz has a support specific surface area of 0.1 m^2/g as specified by the supplier. Due to the low surface area this value could not be reliably verified due to the measurement error of nitrogen physisorption. The fumed silica materials have surface areas ranging from 50 to 380 m^2/g. Note the low specific surface area of the silylated supports compared to the hydrophilic counterparts (entries SiO_2_300, $MeSiO_2$_260 and $MeSiO_2$_260-ht). These are expected to have similar specific surface areas since the hydrophobic silica (support used in sample $MeSiO_2$_260) is obtained via silylation of the hydrophilic silica (a 300 m^2/g Aerosil) and $MeSiO_2$_260-ht is prepared by a heat treatment of $MeSiO_2$_260. The slight gain in specific surface area after converting hydrophobic ($MeSiO_2$_260) into hydrophilic ($MeSiO_2$_260-ht) silica suggests that for the hydrophobic silica the organic species are blocking part of the pores.

The density of hydroxyl species is slightly higher for the alumina than for the silica supports in Table 1, while the differences between the crystalline and amorphous silica materials are small [54,61]. It must be said that the determination of the exact number of surface species is difficult for materials with such low specific surface area and can differ significantly based on the preparation procedure [54]. It is expected that the density of these species is lower on crystalline surface as the more reactive species are condensed [54,61]. When the amorphous silica materials are silylated in order to block the surface hydroxyl species ($MeSiO_2$_110 and $MeSiO_2$_260), a sharp decrease in the density of hydroxyl species is observed (compared untreated to Aerosil material). This significant drop in hydroxyl density is expected because these species have reacted with the silylating agent, resulting in inert siloxy groups. The catalyst supported on quartz (SiO2_0.1) does differ in chemical nature from the rest of the silica samples but acts as a low surface silica which can be compared with the low surface area α-alumina catalysts.

The catalysts tabulated in Table 1 have a wide range of support specific surface area (0.1 – 380 nm^2), while the metal weight loading and silver particle sizes are very similar. This is achieved by carefully adjusting the heat treatment conditions during catalyst preparation, as was more extensively discussed in a previous publication [31]. In previous studies large variations in support properties were always accompanied by different particle sizes. In our case we have been able to tune the particle size to a limited range for which we reported earlier that variations within this particle size range are not expected to significantly affect the selectivity [31]. This allows to attribute observed differences in catalytic results as discussed in the next section solely to the differences in chemical nature and specific surface area of the support material.

Table 1
Catalysts with support characteristics and average metal particle sizes.

Catalyst	Support material		Specific surface area support (m^2/g)		Density of hydroxyl species (OH nm^{-2})	Ag particle size (nm)	
	Brand name	Type	Provided by supplier	Nitrogen physisorption		TEM/SEM ± sigma	UV/Vis (SPR Peak position)‡
Al_2O_3_1	N/A	α-alumina	1	< 5	6 [54,55]	71 ± 25	70 (457)
Al_2O_3_8	AL4196E	α-alumina	8	n.d.	6 [54,55]	77 ± 22	72 (463)
Al_2O_3_20	N/A	α-alumina	N/A	20*	n.d.	n.d.	80 (480)
SiO_2_0.1	N/A	Quartz	0.1	< 1	< 3 [56,57,58]	110 ± 70	108 (503)
SiO_2_50	Aerosil OX50	Fumed silica	50	46	3 [53]	60 ± 15	70 (455)
SiO_2_200	Aerosil 200	Fumed silica	200	196	3 [53]	42 ± 9	41 (401)
SiO_2_380	Aerosil 380	Fumed silica	380	315	3 [53]	34 ± 11	41 (400)
$MeSiO_2$_110	Aerosil R972	Hydrophobic fumed silica	110	97	0.71 [59]	68 ± 33	71 (435)
$MeSiO_2$_260	Aerosil R812	Hydrophobic fumed silica	260	225	0.44 [60]	79 ± 39	77 (485)
$MeSiO_2$_260-ht	N/A	Heat treated Hydrophobic fumed silica	N/A	278	n.d.	n.d.	77 (485)

‡ Peak maximum of surface plasmon resonance peak in diffuse reflectance UV/Vis spectroscopy.
* Support specific surface area as determined by mercury intrusion.

3.2. Catalysis

The temperature dependent catalytic performance of two catalysts (Al_2O_3_1 and SiO_2_200) is shown in Fig. 3. We selected these two examples as the specific support surface and nature of these two catalysts differ greatly. The oxidation of ethylene starts around 170 °C with similar activity over the whole temperature range for these two catalysts (left frame Fig. 3). In the middle frame, the selectivities are plotted versus the reaction temperature. Selectivities toward ethylene oxide range from 40 to 75% for the α-alumina supported catalyst. For the silica supported catalyst the selectivies are clearly lower, ranging from 20 to 50%. In the right frame of Fig. 3, the Arrhenius plots show the activation energy for the epoxidation reaction for both catalysts, based on the yield of ethylene oxide (the explanation for this method can be found in the Supporting information section D). The apparent activation energies for ethylene oxide formation of 74 and 67 kJ/mol for catalysts supported on silica and alumina respectively are well in line with the activation energies reported in literature, which range from 50 to 80 kJ/mol [35,46,62,63].

The remarkably similar conversions over the entire temperature range in the left frame of Fig. 3 strongly suggests that neither the nature of the support nor the silver surface density ($Ag/m_{support}^2$) influence the activity of the catalyst. The very similar activation energies observed on the two totally different supports as represented in the right frame of Fig. 3 imply that the same is true for the rate r_1; and since the overall ethylene conversions are nearly identical, this also applies to r_2. First of all, this shows the accuracy and reproducibility of the measurements. The same metal precursors and solvents were used in the preparation of all catalysts. The results validate our starting point that our preparation method leads to Ag nanoparticles that are very similar in properties, despite being prepared on very different supports in terms of chemistry and surface area. Furthermore, it validates the assumption that the oxidation reaction of ethylene occurs solely on the silver particles, and that the primary selectivity (which fraction of ethylene is converted to the desired product, and which fraction is combusted) is independent of the support used.

The overall selectivity in the middle frame shows a very different picture, with a much higher selectivities for the low surface area α-alumina than for the high surface area silica supported catalyst. This confirms earlier reports of support-dependence of the selectivity and is attributed to a secondary selectivity loss mechanism via subsequent oxidation of the formed ethylene oxide. It is likely that the isomerization of ethylene oxide ($r_{3,a}$) is catalyzed by surface groups of the support. The subsequent oxidation of acetaldehyde ($r_{3,b}$) is assumed to occur on the silver particles rather than on the support surface, and hence is expected to occur with a similar rate for all catalysts. The decreasing selectivity with increasing conversion, as shown in the middle frame, has been reported before [33,39], stating a linear or first order correlation [21,33,36,64]. However, no chemical or physical explanation for this relation has been given. In the following section we try to describe and understand the dependence of selectivity on support properties and conversion. For a direct comparison of the selectivity, catalytic performance should be compared at similar conversion instead of at different temperatures, to exclude the contribution of differences in activation energies due to the different temperatures. Hence, all further measurements discussed in this paper are obtained at a constant

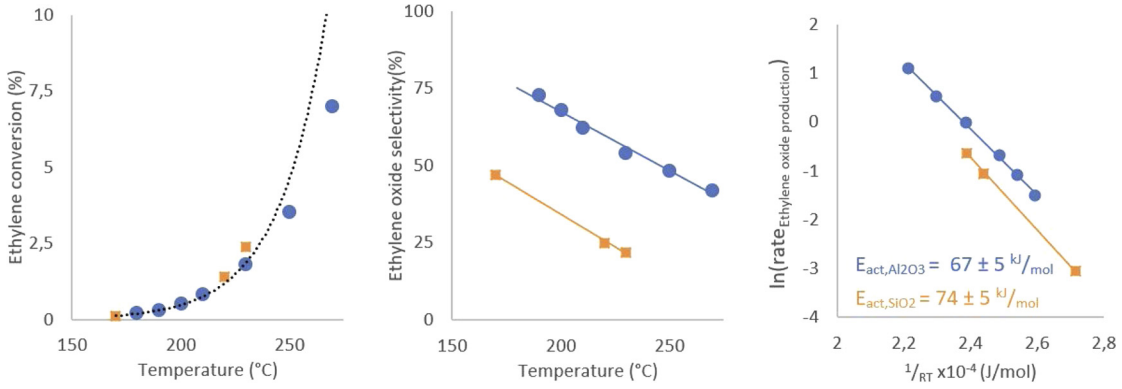

Fig. 3. Conversion (left), selectivity (mid) and Arrhenius plots (right) for the formation of ethylene oxide of Ag_Al2O3_1 (blue circles) and Ag_SiO2_200 (orange squares) measured at a GHWV of 43 L g_{Ag}^{-1} hr^{-1} at atmospheric pressure. Lines added to guide the eye. (For interpretation of the references to colour in this figure legend, the reader is referred to the web version of this article).

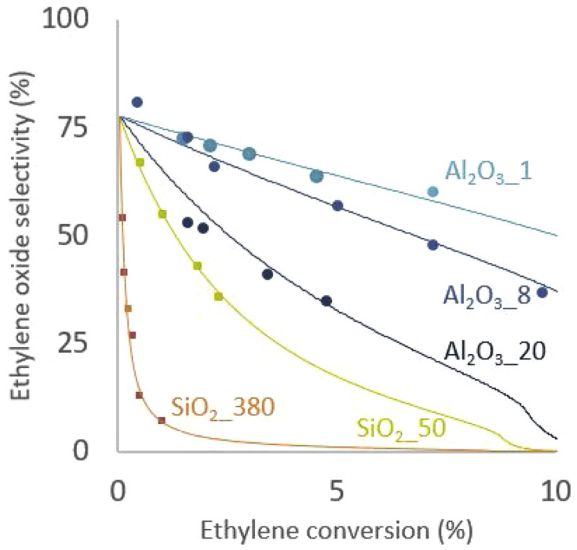

Fig. 4. Selectivity of a selection of catalysts over a 0–10 % range of ethylene conversions showing a support specific surface area and conversion dependent selectivity. Markers correspond to averaged conversion and selectivity obtained after at least 2 h of steady state operation after setting the GHWV. All data is obtained at an operating temperature of 180 °C. Different conversion were obtained over a range of 25–160 hr^{-1} GHWV. Drawn lines correspond to first order fit of catalytic data using the method described.

temperature of 180 °C, and desired conversions were obtained by changing the gas hourly weight velocity (GHWV) rather than the temperature.

3.3. Influence of the conversion on the selectivity

In Fig. 4, the selectivity to ethylene epoxide as a function of ethylene conversion is shown for a selection of catalysts (Similar plots for the other samples can be seen in Figure I1 in the Supporting information). Only results up to 10% conversion are displayed, as for higher conversions mass transfer limitations start to play a major role (see Supporting information section F for the calculation of the expected mass transfer effects). Striking is that, although the selectivities vary widely, at the lowest possible conversions measured all selectivities converge to a similar value (around 76%). This implies a metal specific, intrinsic primary selectivity, which is independent on the type and the specific surface area of the support, and hence determined solely by the silver metal.

Another general observation is that the low surface area alumina-supported catalysts exhibit significantly higher selectivities than the catalyst with the highest support specific surface area, SiO_2_380. Also within the family of alumina-supported catalysts, there is a clear correlation with specific surface area, with decreasing selectivity with larger surface area. This trend of decreasing selectivity with increasing surface area also holds for all the hydrophilic silica supported samples (Figure I1 in Supporting information).

It has been reported before that the selectivity of this process generally decreases with increasing conversion, but there are no earlier reports on the exact dependence. Based on empirical correlations for low-surface area alumina-supported catalysts, such as Al_2O_3_1 in Fig. 4, a linear dependence is assumed, without a theoretical framework to explain this linearity. However, from our results it is clear there is no simple linear correlation, but that in fact the correlation is more complicated. Considering the overall reaction steps describe earlier in this work, it can be expected that the selectivity is inversely dependent on the ethylene oxide partial pressure. As with increasing ethylene oxide partial pressure, the rate r_3 increases. While this trend is well accepted and provides a satisfactory qualitative description of the dependencies of the selectivity with conversion and support specific surface area, the mechanism of this secondary reaction is not extensively studied and a linear decay with conversion is often presumed. In the following section we will discuss a precise model to describe the catalytic data, and the dependence of selectivity on conversion and support properties, allowing more insight in the underlying mechanisms and providing a quantitative description of the rate of the secondary reaction.

3.4. Quantitative description and understanding of the selectivity trends

Our model to describe the experimental results consists of two parallel and one consecutive reaction (with rates r_1, r_2 and r_3 respectively) and is given in Equations 1-4. In these equations the partial pressures of the relevant compounds ethylene, oxygen, ethylene oxide and acetaldehyde are represented as $p_{C_2H_4}$, p_{O_2}, p_{EO} and p_{AA} respectively. The rationale for the reaction orders in r_1 and r_2 is explained in the experimental section. The primary selectivity is determined by the balance between the two possibilities for the oxidation of ethylene: selective oxidation forming the desired product ethylene oxide (r_1) and full oxidation to form carbon dioxide and water (r_2). The ethylene oxide product can either be retrieved or oxidized further in the reactor (r_3). This secondary reaction involves isomerisation of ethylene oxide to acetaldehyde ($r_{3,a}$) and subsequent full oxidation of the isomer, yielding carbon dioxide and water ($r_{3,b}$). Isomerisation to acetaldehyde is considered the rate limiting step [18,21,22], hence the rate of $r_{3,b}$ is considered to be infinitely fast, and the overall reaction rate r_3 can be taken as equal to $r_{3,a}$, and is modelled as a first order rate equation. The rates of the three reactions r_1, r_2 and $r_{3,a}$, were obtained from fitting the experimental data.

$$r_1 = k_1 p_{C_2H_4} p_{O_2}^{\frac{1}{2}} \quad (1)$$

$$r_2 = k_2 p_{C_2H_4}^{\frac{1}{2}} \quad (2)$$

$$r_{3,a} = k_{3,a} p_{EO} \quad (3a)$$

$$r_{3,b} = k_{3,b} p_{O_2}^{n} p_{AA}^{m} \quad (3b)$$

$$\text{if } r_{3,a} \gg r_{3,b}$$

$$r_3 \approx k_3 p_{EO} \quad (4)$$

We considered the experimentally obtained selectivities as a function of conversion for all catalysts presented in Table 1. The drawn lines in Fig. 4 represent the calculated selectivities versus conversion for a selection of these catalysts. Our experimental results clearly showed that at very low ethylene conversions (and hence negligible ethylene oxide concentrations) results for all our supported silver catalysts converge to the same selectivity of 76%. This is in line with earlier reports that at constant conversion there is no intrinsic effect of particle size on selectivity [31]. From this value, which represents the metal specific selectivity, the ratio between r_1 and r_2, and hence k_1 and k_2 was derived. The average value of the k_1/k_2 values derived from the extrapolation of all individual catalysts in the dataset was used as a fitting constraint for the rate constants of the r_1 and r_2 reactions for all samples.

We took a fixed value for the orders of reactions r_1 and r_2, but in fact the variation in oxygen partial pressure does influence the reaction order of both oxygen and ethylene in the r_1 and r_2 reactions [45–47,65]. To justify our simplification, we performed a robustness test in which the same calculations were performed with oxygen reaction orders over the ranges mentioned in literature (-0.5 to 1.5 in oxygen and 1 in ethylene for r_1 and -1 to 1 in oxygen and 0 in ethylene for r_2) [27,45–47]. The reaction orders in r_1 and r_2 did not significantly influence the shape of the fitted curve but did change the absolute value of k_3. This did not influence the capability of the model to fit the data, as the relative values did not change. The higher reaction orders in

oxygen (above 0 and 0.5 for r_1 and r_2 respectively) could not adequately describe the experimental data. These observations support our hypothesis that the orders in both oxygen and ethylene in r_1 and r_2 are not determining factors in our assessment of the role of the support on the r_3-reaction. Moreover, at industrially relevant and non-mass transfer limited conversions, the partial pressures of oxygen and ethylene do not significantly change and therefore only play an indirect role.

It is clear from Fig. 4 that our model is capable of adequately describing the overall decreasing selectivity with increasing conversion. Also, the absolute selectivities calculated using our model correlate well with the measured values for all catalysts. As the rate orders in r_1 and r_2 did not have a large influence on these data, it can be concluded that the good correlation between the measurement and the calculated data is primarily determined by the r_3 reaction, the isomerization of ethylene oxide. From the decrease in selectivity with increasing conversion, for each catalyst a value for k_3, was derived, which depended on the nature and surface area of the support and is discussed in detail in the following section. The strong dependence on the support led to the conclusion that the rate limiting step for the oxidation of ethylene oxide, the isomerization of ethylene oxide to acetaldehyde, occurs over the catalyst support, rather than on the metal surface as is an often proposed theory [21,46,66]. As stated before at low ethylene conversions the support has no influence on selectivity, hence selective (r_1) and full oxidation of ethylene (r_2) can therefore be assumed to solely occur on the surface of the metal particle.

As an illustration of how well the model is able to describe the experimental selectivities, it is interesting to have a close look, at the sharp drop in selectivity for the Al_2O_3_20 sample in Fig. 4 at a conversion of circa 9%, which is correctly predicted with our model. As the unselective reactions r_2 and r_3 consume more oxygen than the selective reaction (r_1), the atmosphere is deprived of oxygen at low selectivities and high conversions (Figure G1 in the Supporting information). In the case of Al_2O_3_20, the resulting oxygen partial pressure is very low (< 0.0034 atm compared to 0.085 atm in the feed, which corresponds to an oxygen conversion of 96%). This drop is correctly described in our model by the positive reaction order in oxygen for the selective r_1 reaction while the reaction order in oxygen for full oxidation r_2 reaction is zero. These orders reflect the fact that a more oxidized silver surface favors the selective oxidation, and hence at these very low oxygen contents the full oxidation reactions are more dominant [27,67]. As the reaction follows the Mars-Van Krevelen type mechanism, these low oxygen contents are insufficient to reoxidize the surface. At the sites where these “oxygen vacancies” exist, the underlying silver is exposed which acts as an active site for the unselective r_2 reaction, the reduced rate of reoxidation causes a sharp drop in the selectivity towards ethylene oxide [68].

3.5. Influence of the nature and specific surface area of the support

The data in Fig. 4 clearly show that the specific surface area of the support has a strong influence on the selectivity, but also the chemical nature of the support seems to play a role. To unravel these two factors, the values for k_3 obtained from all catalysts mentioned in Table 1 (catalytic data in Figures I1) were plotted versus the specific surface of the support materials (Fig. 5). To minimize the error originating from slight differences in overall activity, the obtained k_3 values were divided by the corresponding value for k_1 obtained from the fit. A high value for k_3 corresponds to a low selectivity while a low value corresponds to a very selective catalyst.

The three α-alumina supported catalysts are plotted in blue. These catalysts have a low support specific surface and low values for k_3/k_1 (hence high selectivities). The silica supported samples are depicted in orange, these catalysts have a wide range of support specific surface areas and values for k_3/k_1. The silica-supported catalyst with the lowest support specific surface area, the quartz supported SiO_2_0.1, is an outlier with a higher k_3/k_1 ratio than expected. We tentatively explain

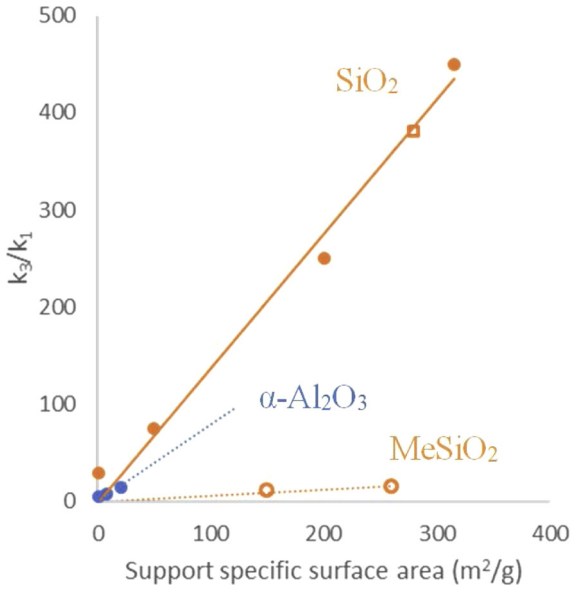

Fig. 5. k_3/k_1 obtained from fitting catalytic data of supported silver catalysts grouped by support material (α-alumina in blue and silica in orange) versus support specific surface area. Open symbols corresponding to silylated silica with the heat-treated sample (alkyl surface groups removed again) indicated by a square. Trendlines are added to guide the eye, these lines are forced through the origin and the dashed lines are extrapolated to more clearly indicate the differences in the slope of the different families. (For interpretation of the references to colour in this figure legend, the reader is referred to the web version of this article).

this by a relatively large error in the exact value for the specific surface area value (provided by supplier). The open symbols correspond to the catalysts supported on surface-treated silica with intermediate to high SSA, but low values for k_3/k_1. $MeSiO_2$_260-ht is depicted as the open square, with k_3/k_1 in line with the untreated silica. For both the alumina and silica supported catalysts, the data were accurately described with a linear relation between the rate constant and specific surface area of the support. The slope depends strongly on the type of material, with a larger slope for the silica than for the alumina-supported and hydrophilic silica catalysts.

Fig. 5 shows that the rate constant of isomerization is proportional to the specific surface area, but only for a given support. Deviations from the linear regression are small and can be ascribed to the experimental error in the fit by the model. However, a non-zero rate of isomerization in the absence of support material could also be considered. Possibly due to some minor isomerization occurring over the metal particle [21,46,66]. This is an interesting topic for future investigations, but not considered further in this work. Mind that the rate constant of the isomerization of the product ethylene oxide to acetaldehyde, k_3, is not a true rate constant of an elementary reaction. Assuming that within a set of materials, the surface density of the active surface groups can be considered constant [53], this linear relation suggests that the reaction can be considered as a first order reaction in the concentration of active surface species. Fig. 5 also shows that the slope is higher for silica than α-alumina. However, this cannot be explained just based on the surface concentration of hydroxyl species on each material (see Table 1) [54–60,69]. This suggests that the hydroxyl species on α-alumina are more reactive than the hydroxyl species on silica supports. This provides an explanation for the observations of Lee and Yong, who state that silica support materials are relatively inert [20,66], and Chongterdtoonskul and Goncharova stating that high surface area of their alumina samples yield overall low selectivities [70,71].

As the strength and the amount of the active species play a role, the observations of Lee and Yong and Chongterdtoonskul and Goncharova

could both be explained by variations of these two parameters in the material. In Figure J1 in the Supporting information, we have tested a set of catalysts on low surface area support with relatively acidic surface species, such as niobia and strontiumtitanate. These types of supports are reported to be very selective by Chongtertoonskul [71,72]. In our case, these catalysts exhibited selectivities towards ethylene oxide similar to a silica catalyst with a specific surface area of 380 m^2/g for the niobia supported catalyst and 70 m^2/g for the strontiumtitanate sample (Figure J1 in the Supporting information), while both have a specific surface area lower than 20 m^2/g. This is in accordance to the observations of both Lee and Yong, where acidic support materials exhibit lower selectivities towards ethylene oxide [20,24]. We attribute this to a higher rate of ethylene oxide isomerization over acidic support species.

A very striking and interesting feature in Fig. 5 are the low k_3/k_1 values for $MeSiO_2$-110 and $MeSiO_2$-260. While the support specific surface area of these materials is comparable to the other silica supported samples, the selectivity towards ethylene oxide is much higher; the decrease in the k_3/k_1 value is 96%. This means that the 260 m^2/g silica supported catalyst has a similar catalytic performance to a 20 m^2/g α-alumina catalyst. In this sample the original silanol groups are blocked by organic species. When these alkyl groups were burned off by heat treatment (square in Fig. 5), the sample, $MeSiO_2$-260-ht, had a k_3/k_1 value similar to a catalyst supported on untreated silica with a similar specific surface area. This clearly shows that the difference in selectivity can be solely attributed to the difference in the support material, in this case the chemical nature of the surface.

4. Conclusion

Supported catalysts with silver particle sizes of 40–70 nm were prepared on silica and α-alumina supports with varying specific surface areas. The silver weight-based activity of the catalysts was similar for all catalysts. However, the selectivity in the ethylene epoxidation, the most critical factor, depended strongly on the support and on the conversion. Although it was known in the literature that the selectivity decreased with increasing conversion, this effect had not been described in detail. Using a kinetic model, we could accurately describe the catalytic selectivity of our range of supported silver catalysts and conversions. Even seemingly surprising features, such as a sudden drop in selectivity at relatively high conversions due to a low oxygen content, was faithfully modeled. Our data fully supported that the primary selectivity (at very low conversions) is governed by the two alternative reaction paths for the ethylene reactant on the silver catalyst surface, while a further loss of selectivity at higher conversions is caused by a secondary reaction involving the support surface, most likely ethylene oxide isomerization to acetaldehyde followed by complete combustion.

Building on the hypothesis of a first order in ethylene oxide for this secondary reaction, the rate constants were shown to be linearly dependent on the support specific surface area but differed per material type. The presumed active site for the isomerization reaction are hydroxyl groups, and the proportionality suggests a first order in the hydroxyl species. The difference in rate constant for either silica or α-alumina did not simply scale with the hydroxyl density on these supports, so probably the rate of isomerization does also depend on the specific properties of the surface sites.

We clearly showed that the loss of selectivity with increasing conversion depends directly on the density of active surface groups, and hence specific support surface area. In this paper, we kept the weight loading similar to the low surface area supported catalysts, but in industry, one would ideally be able to use a high surface area support (and hence silver loading and volume activity) without losing too much selectivity. We showed that passivation of the silanol groups of a high surface area silica support, led to a selective, high surface area catalyst. The selectivity to ethylene oxide for this catalyst supported on modified silica was similar to that of an α-alumina supported catalyst with ten times lower specific surface area. High surface area supports allow to increase the silver weight loading, potentially leading to even higher selectivities as the metal is expected to block reactive hydroxyl species on the surface and to the possibility to load more active catalyst surface per reactor volume. Alternatively, these materials could be used to produce more stable catalysts as the high interparticle distance increases the stability against deactivation due to sintering.

Acknowledgements

This research was founded by NWO Vici project 16.130.344. The authors would like to thank Jan-Willem de Rijk, Carlo Buijs (SCR Technical University Eindhoven) and Marlies Coolen-Kuppens (SCR Technical University Eindhoven) for their help on the epoxidation setup and Marjan Versluijs-Helder for SEM and TGA measurements.

Appendix A. Supplementary data

Supplementary data associated with this article can be found, in the online version, at https://doi.org/10.1016/j.cattod.2019.04.049

References

[1] S. Rebsdat, D. Mayer, Ethylene oxide, Ullmann's Encycl. Ind. Chem. Wiley-VCH Verlag GmbH & Co, KGaA, Weinheim, Germany, 2001, pp. 547–572, https://doi.org/10.1002/14356007.a10_117.
[2] Research In China, Global and China Ethylene Oxide (EO) Industry Report, 2017-2021, (2017), pp. 1–137 https://www.reportbuyer.com/product/5013139/global-and-china-ethylene-oxide-eo-industry-report-2017-2021.html.
[3] H. van Milligen, B. VanderWilp, G.J. Wells, Enhancements in Ethylene Oxide / Ethylene Glycol Manufacturing Technology, (2016).
[4] J.C. Zomerdijk, M.W. Hall, Technology for the manufacture of ethylene oxide, Catal. Rev. 23 (1981) 163–185, https://doi.org/10.1080/03602458108068074.
[5] H. Kestenbaum, A. Lange de Oliveira, W. Schmidt, F. Schüth, W. Ehrfeld, K. Gebauer, H. Löwe, T. Richter, D. Lebiedz, I. Untiedt, H. Züchner, Silver-catalyzed oxidation of ethylene to ethylene oxide in a microreaction system, Ind. Eng. Chem. Res. 41 (2002) 710–719, https://doi.org/10.1021/ie010306u.
[6] E. Alper, O. Yuksel Orhan, CO 2 utilization: developments in conversion processes, Petroleum 3 (2017) 109–126, https://doi.org/10.1016/j.petlm.2016.11.003.
[7] H.L. Greenberg, M.G. Ott, R.E. Shore, Men assigned to ethylene oxide production or other ethylene oxide related chemical manufacturing: a mortality study, Br. J. Ind. Med. 47 (1990) 221–230, https://doi.org/10.1136/oem.47.4.221.
[8] P.P. Mcclellan, Manufacture and uses of ethylene oxide and ethylene glycol, Ind. Eng. Chem. (1950) 2402–2407, https://doi.org/10.1021/ie50492a013.
[9] R.A. Sheldon, The e factor: fifteen years on, Green Chem. 9 (2007) 1273, https://doi.org/10.1039/b713736m.
[10] T.E. LeFort, Process for the production of ethylene oxide, US 1998878 A, 1935.
[11] G.A. Perkins, Dichlobomksii ethees, US2042862, 1936.
[12] J.M. Kobe, W.E. Evans, R.L. June, M.F. Lemanski, Epoxidation, Encycl. Catal. (2003) 246.
[13] M.J.F.M. Verhaak, Process for the production of ethylene oxide, US8969602B2, 2015.
[14] R. van Santen, Catalysis in perspective: historic review, Catal. From Princ. to Appl. (2012), pp. 3–19 doi:978-3-527-32349-4.
[15] M.O. Ozbek, I. Onal, R.A. Van Santen, Ethylene epoxidation catalyzed by chlorine-promoted silver oxide, J. Phys. Condens. Matter 23 (2011) 404202–404209, https://doi.org/10.1088/0953-8984/23/40/404202.
[16] J.T. Jankowiak, M.A. Barteau, Ethylene epoxidation over silver and copper–silver bimetallic catalysts: I. Kinetics and selectivity, J. Catal. 236 (2005) 366–378, https://doi.org/10.1016/j.jcat.2005.10.018.
[17] R.P. Nielsen, J.H. La Rochelle, Catalyst for production of ethylene oxide, US3962136, 1976.
[18] M.O. Ozbek, I. Onal, R.A. van Santen, Why silver is the unique catalyst for ethylene epoxidation, J. Catal. 284 (2011) 230–235, https://doi.org/10.1016/j.jcat.2011.08.004.
[19] G.H. Twigg, The mechanism of the catalytic oxidation of ethylene. I. Experiments using a flow system, Proc. R. Soc. A Math. Phys. Eng. Sci. 188 (1946) 92–104, https://doi.org/10.1098/rspa.1946.0099.
[20] J.K. Lee, X.E. Verykios, R. Pitchai, Support participation in chemistry of ethylene oxidation on silver catalysts, Appl. Catal. 44 (1988) 223–237, https://doi.org/10.1016/S0166-9834(00)80055-X.
[21] O.O. Bernardini, E.A. Cherniak, Heterogeneous isomerization of ethylene oxide to acetaldehyde, Can. J. Chem. 51 (1972) 1371–1377.
[22] C.-F. Mao, M. Albert Vannice, High surface area α-aluminas III. Oxidation of ethylene, ethylene oxide, and acetaldehyde over silver dispersed on high surface area α-alumina, Appl. Catal. A Gen. 122 (1995) 61–76, https://doi.org/10.1016/0926-860X(94)00214-2.
[23] D.A. Bulushev, E.A. Paukshtis, Y.N. Nogin, S. Bal, Transient response and infrared studies of ethylene oxide reactions on silver catalysts and supports, Appl. Catal. A

Gen. 123 (1995) 301–322.
[24] Y. Yong, E.M. Kennedy, N.W. Cant, Oxide catalysed reactions of ethylene oxide under conditions relevant to ethylene epoxidation over supported silver, Appl. Catal. 76 (1999) 31–48.
[25] M.C.N.A. Carvalho, C.A. Perez, R.A. Simão, F.B. Passos, M. Schmal, The promoting effect of cesium on structure and morphology of silver catalysts, An. Acad. Bras. Cienc. 76 (2004) 19–27, https://doi.org/10.1590/S0001-37652004000100003.
[26] A.M. Lauritzen, Ethylene Oxide Catayst and Process for Preparing the Catalyst, US4761394, 1988.
[27] M.O. Özbek, R.A. van Santen, The mechanism of ethylene epoxidation catalysis, Catal. Lett. 143 (2013) 131–141, https://doi.org/10.1007/s10562-012-0957-3.
[28] J. Wang, P.D. Ellis, Cesium-induced structural change of adsorbed ethylene on cesium-promoted silver catalyst studied by13C solid-state nuclear magnetic resonance, J. Am. Chem. Soc. 113 (1991) 9675–9676, https://doi.org/10.1021/ja00025a044.
[29] S. Linic, M.A. Barteau, On the mechanism of Cs promotion in ethylene epoxidation on Ag, J. Am. Chem. Soc. 126 (2004) 8086–8087, https://doi.org/10.1021/ja048462q.
[30] R.M. Carter, Process for the preparation of ethylene oxide, US2294383, 1946.
[31] J.E. van den Reijen, S. Kanungo, T.A.J. Welling, M. Versluijs-Helder, T.A. Nijhuis, K.P. de Jong, P.E. de Jongh, Preparation and particle size effects of Ag/a-Al2O3 catalysts for ethylene epoxidation, J. Catal. 356 (2017) 65–74, https://doi.org/10.1016/j.jcat.2017.10.001.
[32] H.R. Dettwiler, A. Baiker, W. Richarz, Kinetics of ethylene oxidation on a supported silver catalyst, Helv. Chim. Acta 62 (1979) 1689–1700, https://doi.org/10.1002/hlca.19790620602.
[33] Y.C. Kim, N.C. Park, J.S. Shin, S.R. Lee, Y.J. Lee, D.J. Moon, Partial oxidation of ethylene to ethylene oxide over nanosized Ag/α-Al2O3 catalysts, Catal. Today 87 (2003) 153–162, https://doi.org/10.1016/j.cattod.2003.09.012.
[34] M.A. Al-Juaied, D. Lafarga, A. Varma, Ethylene epoxidation in a catalytic packed-bed membrane reactor: experiments and model, Chem. Eng. Sci. 56 (2001) 395–402, https://doi.org/10.1016/S0009-2509(00)00235-9.
[35] D. Lafarga, M.A. Al-juaied, C.M. Bondy, A. Varma, Ethylene epoxidation on Ag-Cs / α-Al2O3 catalyst : experimental results and strategy for kinetic parameter determination, Ind. Eng. Chem. Res. 39 (2000) 2148–2156, https://doi.org/10.1021/ie990939x.
[36] R.E. Kenson, M. Lapkin, Kinetics and mechanism of ethylene oxidation. Reactions of ethylene and ethylene oxide on a silver catalyst, J. Phys. Chem. 74 (1970) 1493–1502, https://doi.org/10.1021/j100702a017.
[37] J.K. Lee, X.E. Verykios, R. Pitchai, Support and crystallite size effects in ethylene oxidation catalysis, Appl. Catal. 50 (1989) 171–188, https://doi.org/10.1016/S0166-9834(00)80834-9.
[38] Y. Hui-Xing, C. Hua, H. De-Gang, The rate constant determination for the isomerization of ethylene oxide to acetaldehyde by chemical shock tube, Acta Chim. Sin. (1989) 941–946.
[39] J.E. van den Reijen, P.H. Keijzer, P.E. de Jongh, Pore structure stabilization during the preparation of single phase ordered macroporous α-alumina, Materialia 4 (2018) 423–430, https://doi.org/10.1016/j.mtla.2018.10.016.
[40] S.M. Pourmortazavi, S.S. Hajimirsadeghi, I. Kohsari, R. Fareghi Alamdari, M. Rahimi-Nasrabadi, Determination of the optimal conditions for synthesis of silver oxalate nanorods, Chem. Eng. Technol. 31 (2008) 1532–1535, https://doi.org/10.1002/ceat.200800090.
[41] A.R. Fiorucci, L.M. Saran, É.T.G. Cavalheiro, E.A. Neves, Thermal stability and bonding in the silver complexes of ethylenediaminetetraacetic acid, Thermochim. Acta 356 (2000) 71–78, https://doi.org/10.1016/S0040-6031(00)00478-0.
[42] V.V. Boldyrev, Thermal decomposition of silver oxalate, Thermochim. Acta 388 (2002) 63–90, https://doi.org/10.1016/S0040-6031(02)00044-8.
[43] E. Plessers, J.E. van den Reijen, P.E. de Jongh, K.P. de Jong, M.B.J. Roeffaers, Origin and abatement of heterogeneity at the support granule scale of silver on silica catalysts, ChemCatChem. 9 (Dec(24)) (2017) 4562–4569, https://doi.org/10.1002/cctc.201700753.
[44] J. Hoekstra, A.M. Beale, F. Soulimani, M. Versluijs-Helder, J.W. Geus, L.W. Jenneskens, Shell decoration of hydrothermally obtained colloidal carbon spheres with base metal nanoparticles, New J. Chem. 39 (2015) 6593–6601, https://doi.org/10.1039/C5NJ00804B.
[45] C.T. Campbell, M.T. Paffett, Model studies of ethylene epoxidation catalyzed by the Ag(110) surface, Surf. Sci. 139 (1984) 396–416, https://doi.org/10.1016/0039-6028(84)90059-1.
[46] C. Stegelmann, N.C. Schiødt, C.T. Campbell, P. Stoltze, Microkinetic modeling of ethylene oxidation over silver, J. Catal. 221 (2004) 630–649, https://doi.org/10.1016/j.jcat.2003.10.004.
[47] S. Linic, M.A. Barteau, Construction of a reaction coordinate and a microkinetic model for ethylene epoxidation on silver from DFT calculations and surface science experiments, J. Catal. 214 (2003) 200–212, https://doi.org/10.1016/S0021-9517(02)00156-2.
[48] P. Harriott, The oxidation of ethylene using silver on different supports, J. Catal. 21 (1971) 56–65, https://doi.org/10.1016/0021-9517(71)90120-5.
[49] P.L. Metcalf, P. Harriott, Kinetics of silver-catalyzed ethylene oxidation, Ind. Eng. Chem. Process Des. Dev. 11 (1972) 478–484, https://doi.org/10.1021/i260044a004.
[50] D.L. Trimm, Thermal stability of catalyst supports, Catal. Deactiv. (1991) 29–51.
[51] M.M. Martín-Ruiz, L.A. Pérez-Maqueda, T. Cordero, V. Balek, J. Subrt, N. Murafa, J. Pascual-Cosp, High surface area α-alumina preparation by using urban waste, Ceram. Int. 35 (2009) 2111–2117, https://doi.org/10.1016/j.ceramint.2008.11.011.
[52] L.L. Murrell, D.C. Grenoble, J.P. DeLuca, Process for preparing ultra-stable, high surface area alpha-alumina, US4169883, 1976.
[53] Evonik, Aerosil – Fumed Silica: Technical Overview, (2015).
[54] M. Nguefack, A.F. Popa, S. Rossignol, C. Kappenstein, Preparation of alumina through a sol–gel process. Synthesis, characterization, thermal evolution and model of intermediate boehmite, Phys. Chem. Chem. Phys. 5 (2003) 4279–4289, https://doi.org/10.1039/B306170A.
[55] W. Smit, C.L.M. Holten, Zeta-potential and radiotracer adsorption measurements on EFG α-Al2O3 single crystals in NaBr solutions, J. Colloid Interface Sci. 78 (1980) 1–14, https://doi.org/10.1016/0021-9797(80)90489-0.
[56] M.E. Grillo, D.S. Coll, J. Rodríguez, Effect of the environment on the hydroxyl density of α-quartz (111), Chem. Phys. Lett. 522 (2012) 46–50, https://doi.org/10.1016/j.cplett.2011.11.084.
[57] S.M. Pimblott, N.J.B. Green, Recent advances in the kinetics of radiolytic processes, Res. Chem. Kinet. (1993) 117–119.
[58] F.A. Rodrigues, P.J.M. Monteiro, G. Sposito, Alkali-silica reaction the surface charge density of silica and its effect on expansive pressure, Cem. Concr. Res. 29 (1999) 527–530, https://doi.org/10.1016/S0008-8846(98)00220-8.
[59] E. Valencia, A. Maldonado, Adsorption of isobutene on partially hydrophobized aerosil, J. Chem. Soc. Faraday Trans. 86 (1990) 539–543.
[60] J. Warren, S. Offenberger, H. Toghiani, C.U. Pittman, T.E. Lacy, S. Kundu, Effect of temperature on the shear-thickening behavior of fumed silica suspensions, ACS Appl. Mater. Interfaces 7 (2015) 18650–18661, https://doi.org/10.1021/acsami.5b05094.
[61] G.E. Berendsen, L. De Galan, A geometrical model for chemically bonded tms and pds phases, J. Liq. Chromatogr. 1 (1978) 403–426, https://doi.org/10.1080/01483917808060008.
[62] W.M.H. Sachtler, C. Backx, R.A. Van Santen, On the mechanism of ethylene epoxidation, Catal. Rev. 23 (1981) 127–149, https://doi.org/10.1080/03602458108068072.
[63] P. Borman, K. Westerterp, An experimental study of the kinetics of the selective oxidation of ethene over a silver on alpha-alumina catalyst, Ind. Eng. Chem. Res. 34 (1995) 49–58, https://doi.org/10.1021/ie00040a002.
[64] M.J. Palys, S.Y. Ivanov, A.K. Ray, Conceptual approach in multi-objective optimization of packed bed membrane reactor for ethylene epoxidation using real-coded non-dominating sorting genetic algorithm NSGA-II, Int. J. Chem. React. Eng. 15 (2017), https://doi.org/10.1515/ijcre-2016-0041 aop.
[65] R.J. Baxter, P. Hu, Insight into why the Langmuir-Hinshelwood mechanism is generally preferred, J. Chem. Phys. 116 (2002) 4379–4381, https://doi.org/10.1063/1.1458938.
[66] Y.S. Yong, E.M. Kennedy, N.W. Cant, Oxide catalysed reactions of ethylene oxide under conditions relevant to ethylene epoxidation over supported silver, Appl. Catal. 76 (1991) 31–48, https://doi.org/10.1016/0166-9834(91)80003-F.
[67] R.A. Van Santen, H.P.C.E. Kuipers, The mechanism of ethylene epoxidation, J. Adv. Catal. Sci. Technol. (1987) 265–321, https://doi.org/10.1016/S0360-0564(08)60095-4.
[68] M.O. Özbek, I. Önal, R.A. van Santen, Ethylene epoxidation catalyzed by silver oxide, ChemCatChem 3 (2011) 150–153, https://doi.org/10.1002/cctc.201000249.
[69] S. Rojluechai, S. Chavadej, J.W. Schwank, V. Meeyoo, Catalytic activity of ethylene oxidation over Au, Ag and Au-Ag catalysts: support effect, Catal. Commun. 8 (2007) 57–64, https://doi.org/10.1016/j.catcom.2006.05.029.
[70] S.N. Goncharova, E.A. Paukshtis, B.S. Bal'zhinimaev, Size effects in ethylene oxidation on silver catalysts. Influence of support and Cs promoter, Appl. Catal. A Gen. 126 (1995) 67–84, https://doi.org/10.1016/0926-860X(95)00036-4.
[71] A. Chongterdtoonskul, J.W. Schwank, S. Chavadej, Effects of oxide supports on ethylene epoxidation activity over Ag-based catalysts, J. Mol. Catal. A Chem. 358 (2012) 58–66, https://doi.org/10.1016/j.molcata.2012.02.011.
[72] A. Chongterdtoonskul, T. Suttikul, M. Santikunaporn, J.W. Schwank, S. Chavadej, Effect of diluent gas on ethylene epoxidation activity over various Ag-based catalysts on selective oxide supports, J. Mol. Catal. A Chem. 386 (2014) 5–13, https://doi.org/10.1016/j.molcata.2014.02.003.